Materials Research. 2017; 20(3): 639-645
DOI: http://dx.doi.org/10.1590/1980-5373-MR-2015-0373

Analysis of Spinodal Decomposition in Al-Zn and Al-Zn-Cu Alloys Using the Nonlinear Cahn-Hilliard Equation

Victor Manuel Lopez-Hirata [a], Erika Osiris Avila-Davila [b], Maribel-Leticia Saucedo-Muñoz [a], Jose David Villegas-Cardenas [c], Orlando Soriano-Vargas [c]*

[a] *Instituto Politecnico Nacional (ESIQIE) Apartado Postal 118-395, D.F. 07051, Mexico*
[b] *Instituto Tecnológico de Pachuca, Carretera Mexico-Pachuca Km. 87.5 C.P.42080 Pachuca, Hidalgo, Mexico*
[c] *Universidad Politecnica, 54710, Estado de Mexico*

Received: June 22, 2015; Revised: January 29, 2017; Accepted: February 24, 2017

The phase field model based on the nonlinear Cahn-Hilliard equation was applied to analyze the spinodal decomposition process in Al-Zn and Al-Zn-Cu alloys. Partial differential equations were solved using the explicit finite difference method for the Al- 20, and 35 at. % Zn alloys aged at temperatures between 25 and 100 °C for times from 10 s to 2000 s and Al-20at.%Zn-10at.%Cu and Al-20at.%Zn-5at.%Cu alloys at temperatures between 400 and 500 °C for times from 3600 to 360000 s. Thermo-Calc indicated that the copper addition extends the presence of the metastable miscibility gap up to a temperature of about 597 °C in comparison to the temperature of 350 °C for the binary case. This miscibility gap was calculated assuming that the equilibrium phases were not present and thus it is only existing at the early stages of aging. Simulation results pointed out that the phase decomposition process is much faster in the binary alloys than that in the ternary alloys in spite of the higher aging temperature for the latter case.

Keywords: *Microstructural characterization, spinodal decomposition, growth kinetics, Al-Zn and Al-Zn-Cu alloys, phase field method*

1. Introduction

The spinodal decomposition mechanism has been reported[1-3] to occur in the Al-Zn and Al-Zn-Cu alloy systems. Furthermore, this phase transformation is associated with the strengthening of both Al-rich and Zn-rich alloys[4-6]. The spinodal decomposition is also normally related to the presence of a miscibility gap which is present in both Al-Zn and Al-Zn-Cu alloys. In fact, the copper addition has been pointed out[2,3] to increase the temperature of the miscibility gap.

The phase decomposition kinetics in the Al-Zn alloys has been reported[7] to occur very fast in spite of the low aging temperatures. Thus, it has been difficult to study experimentally the spinodal decomposition in the early stages of aging in the binary alloys. To slow the spinodal decomposition kinetics, the addition of copper has been used in several works[2,3].

The phase field method has been successfully applied to analyze the spinodal decomposition in different binary and ternary alloys[8-10] and it seems to be a good alternative to follow the phase decomposition process in both alloys since either short or long aging times can be used to analyze both the early stage of phase decomposition and the coarsening of the decomposed phases.

* e-mail: vlopezhi@prodigy.net.mx

Thus, the purpose of the present work is using the advantage of the phase field method to characterize microstructurally and kinetically the spinodal decomposition in Al-Zn and Al-Zn-Cu alloys aged isothermally for different times in order to understand the effect of the copper addition on the spinodal decomposition process, as well as the difference in the kinetics of phase decomposition and the chemical composition of the decomposed phases.

2. Numerical Methodology

The nonlinear Cahn-Hilliard equation for a multicomponent system with a constant mobility can be reduced to the following equation[8]:

$$\frac{\partial C_i(x \cdot t)}{\partial t} = M\nabla^2\left(\frac{\partial f_0}{\partial C_i} - K_{i,j}\nabla^2 C_i\right) \quad (1)$$

where $c_i(x,t)$ is the concentration of the i element as a function of distance x and time t, M is the atomic mobility, f_o the local free energy, and $K_{i,j}$ the gradient energy coefficient for the solute i in the solvent j.

The local energy f_o was defined using the sub-subregular solution model for the fcc solid solutions, f_o^{cc}, as follows[3]:

$$f_O^{fcc} = X_{Al}f_{Al}^{fcc} + X_{Zn}f_{Zn}^{fcc} + X_{Al}X_{Zn}\sum^{n} L_{Al,Zn}^{fcc}(X_{Al} - X_{Zn})^n \quad (2)$$

And for the ternary alloy system:

$$f_O^{fcc} = X_{Al}f_{Al}^{fcc} + X_{Cu}f_{Cu}^{fcc} + X_{Zn}f_{Zn}^{fcc} + X_{Al}X_{Zn}$$
$$\sum {}^{n}L_{Al,Zn}^{fcc}(X_{Al} - X_{Zn})^n + X_{Al}X_{Cu}$$
$$\sum {}^{n}L_{Al,Cu}^{fcc}(X_{Al} - X_{Cu})^n + X_{Cu}X_{Zn}$$
$$\sum {}^{n}L_{Cu,Zn}^{fcc}(X_{Cu} - X_{Zn})^n \qquad (3)$$

where X_{Al}, X_{Zn} and X_{Cu}, and and f_{Al}, f_{Zn} and f_{Cu} are the molar fraction and free energy of pure Al, Zn and Cu, respectively, and, ${}^{n}L_{Al,Cu}^{fcc}$, ${}^{n}L_{Al,Zn}^{fcc}$ and ${}^{n}L_{Cu,Zn}^{fcc}$ are the interaction parameters for the Redlich-Kister equation[3]. They have a linear function of temperature T according to the following equation:

$${}^{n}L_{i,j}^{fcc} = a_n + b_n T \qquad (4)$$

where a_n and b_n are constants and the exponent n varies from 0 to 3. All these thermodynamic constants are shown in Table 1[3]. Interaction parameters values were determined and kept constant for each alloy composition and temperature.

In the case of the binary Al-Zn alloy system the following nonlinear Cahn-Hilliard equation was utilized for the analysis of phase decomposition:

$$\frac{\partial C_{Zn}(x \cdot t)}{\partial t} = M_{Al,Zn}\nabla^2\left(\frac{\partial f_0}{\partial C_{Al}} - K_{Al,Zn}\nabla^2 C_{Zn}\right) \qquad (5)$$

In contrast, the following two equations were employed to analyze the phase decomposition in the ternary Al-Zn-Cu alloys:

$$\frac{\partial C_{Cu}(x \cdot t)}{\partial t} = M_{Al,Cu}\nabla^2\left(\frac{\partial f_0}{\partial C_{Cu}} - K_{Al,Cu}\nabla^2 C_{Cu}\right) \qquad (6)$$

$$\frac{\partial C_{Zn}(x \cdot t)}{\partial t} = M_{Al,Zn}\nabla^2\left(\frac{\partial f_0}{\partial C_{Zn}} - K_{Al,Zn}\nabla^2 C_{Zn}\right) \qquad (7)$$

That is, these three equations were solved considering periodic boundary condition (same size two-dimension mesh) with a random solute distribution at the initial condition, t=0 s, for all nodes at any x and y coordinate of in order to get the copper and zinc concentrations as a function of position and time. The initial amplitude for the modulation composition was fixed to be about ± 2.0 at. % for the alloying elements in order to produce a very small composition fluctuation.

The atomic mobility M_i is related to the interdiffusion coefficient $\overline{D}_i$ as follows:

$$\overline{D}_{i,j} = M_{i,j}\left(\frac{\partial^2 f_O}{\partial c_i^2}\right) \qquad (8)$$

The atomic mobility M_i was determined using equation (8) and the procedure proposed by Honjo and Saito[8]:

$$M_{Al,Zn} = \frac{D_{Al,Zn}}{2\Omega_{Al,Zn} + 4RT} \qquad (9)$$

$$M_{Al,Cu} = \frac{D_{Al,Cu}}{2\Omega_{Al,Cu} + 4RT} \qquad (10)$$

where $D_{Al\text{-}Zn}$ and $D_{Al\text{-}Cu}$ are the diffusion coefficients of zinc diffusion in aluminum and the diffusion of copper in aluminum, respectively. They are shown in Table 2[11]. The interaction parameter Ω was calculated using the summative expression in Eq. (3) for the Al-Cu or Al-Zn interactions.

The gradient energy coefficient K_i was defined as proposed by Hilliard[12]:

$$K_i = \left(\frac{2}{3}\right)h_{0.5}^{M} r_0^2 \qquad (11)$$

where ${h_{0.5}}^{M}$ is the heat of mixing per unit volume at c = 0.5 and r_o is the nearest-neighbor distance. The gradient energy coefficient K_i was defined as follows:

$$K_{Al-Zn} = \frac{1}{12}{a_{Al}}^2\Omega_{Al-Zn} \qquad (12)$$

$$K_{Al-Cu} = \frac{1}{12}{a_{Al}}^2\Omega_{Al-Cu} \qquad (13)$$

where a_{Al} is the lattice parameter[13] also given in Table 2. The lattice parameter was considered to be constant with respect to temperature during the simulations.

The effect of coherency elastic strain energy has been reported[13] to be very low for the Al-Zn system with an absolute value of the lattice misfit η of about 0.017, and thus it was neglected for the calculation procedure. Nevertheless, the addition of copper in Al-Zn alloys is expected to increase the lattice misfit and thus the coherency elastic strain energy. However, its effect was not considered in the present work because no reliable values of lattice parameters and elastic constants are available for the ternary Al-Zn-Cu alloys.

The equations (5), and (6) and (7) were solved using the explicit finite difference method with 201 x 201 points-square grit with a mesh size of 0.10 nm and a time-step of 0.0001 to 1 s. The initial composition modulation of solute was determined by means of a random-number generator. The node number was selected in order to cover more properly the interface between the decomposed phases. The numerical simulation was carried out in two Al-Zn alloy compositions, 20 and 35at. % Zn, aged at temperatures between 25 and 100 °C for times from 10 s to 2000 s. Zn compositions were chosen in order to be located at the center and extreme of the miscibility gap. In the case of the ternary alloys, two compositions were selected, Al-20at.%Zn-10at.%Cu and Al-20at.%Zn-5at.%Cu, which are close to the Zn composition in the binary alloys. These alloys were numerically simulated at temperatures between 400 and 450 °C for times from 3600 to 360000 s. All these compositions and temperatures were selected in order to be within the coherent spinodal line, which was verified by the increase in the amplitude of composition modulation with aging time during the spinodal decomposition simulation. The equilibrium phase diagrams for the Al-Zn and Al-Zn-Cu alloys were calculated by Thermo-Calc software using pbin and ssol5 data bases[14].

Table 1. Thermodynamic constants for the Al-Cu-Zn system[3]

a_n, b_n J/mole	a_0	b_0	a_1	b	a_2	b_2	a_3	b_3
${}^nL^{fcc}_{Al,Zn}$	7297.48	0.47512	6612.88	-4.5911	-3097.19	3.30635	0	0
${}^nL^{fcc}_{Al,Cu}$	-52290	2	37940	-2	900	0	-1300	0
${}^nL^{fcc}_{Zn,Cu}$	-42803.75	10.02258	2936.39	-3.05323	9034.2	-5.39314	0	0

Table 2. Diffusion coefficients and lattice parameter[11,12]

$D_{Al\text{-}Zn}$ cm^2/s	0.25exp(-113000/RT) R=8.314 J/mole
$D_{Al\text{-}Cu}$ cm^2/s	0.29exp(-130000/RT)
fcc a_{Al} (nm)	0.404 - 0.401

3. Results and Discussions

3.1. Calculated miscibility gaps in Al-Zn and Al-Zn-Cu alloy systems

Figure 1 shows the Thermo-Calc[14] calculated equilibrium Al-Zn phase diagram. A miscibility gap can be observed in this alloy system. It is well known that the supersaturated solution α phase of theses alloys decomposes rapidly into a mixture of only the fcc Al-rich α_1 and Zn-rich α_2 phases as a result of aging either at room temperature or higher temperatures. The complete sequence of precipitation during aging is as follows[15]: first the formation of (Zn-rich) Guinier-Prestone zone, GPZ, spheres with a size of about 1-2 nm, which are completely coherent with the Al-rich α matrix phase. A further aging promotes the change of morphology of GPZ to ellipsoidal one. A subsequent aging causes the formation of the metastable (Zn-rich) α" phase. This is still coherent with the α phase matrix with a size of about 10 nm. A prolonged aging of this type of alloys permits to obtain the equilibrium close packed hexagonal cph (Zn-rich) η phase, which is incoherent with the matrix.

The Al-Cu-Zn miscibility gaps, calculated by Thermo-Calc by considering only fcc phases, at temperatures of 400, 450, 500 and 550 °C are shown in Figure 2. The extension of miscibility gap decreases as the temperature increases. The miscibility gap vanishes at a temperature of about 597 °C which is higher than the maximum temperature of 350 °C in the binary alloy system. This fact suggests that the spinodal decomposition can occur at higher temperatures in the ternary alloy system. Furthermore, Ren et al.[16] pointed out that the copper addition causes an increase in width of the miscibility gap in the Al-Zn system which is in agreement with present work results. These miscibility gaps also indicate that the supersaturated solid solution, α phase, decomposes into a mixture of the Cu-poor Al-Zn α_1 and Cu-rich Al-Zn α_2 phases. The above results are in good agreement with the experimental study reported[2] using binary and ternary diffusion couples carried out at annealing temperatures of 320 and 340 °C.

3.2 Spinodal decomposition process in Al-Zn alloys

The Zn concentration profiles, plot of concentration versus distance, are shown in Figure 3 for the Al-35at.%Zn alloy aged at 50 °C for times from 0 to 1980 s. The total distance was 20 nm, but only a quarter of it is shown to observe more clearly the changes in amplitude. The amplitude of composition modulation increases with aging time as

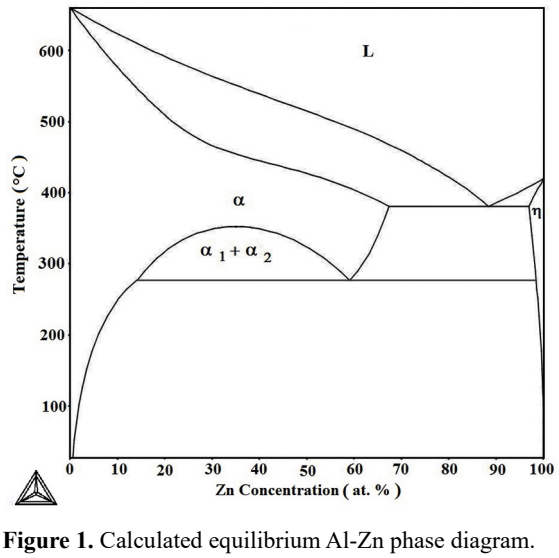

Figure 1. Calculated equilibrium Al-Zn phase diagram.

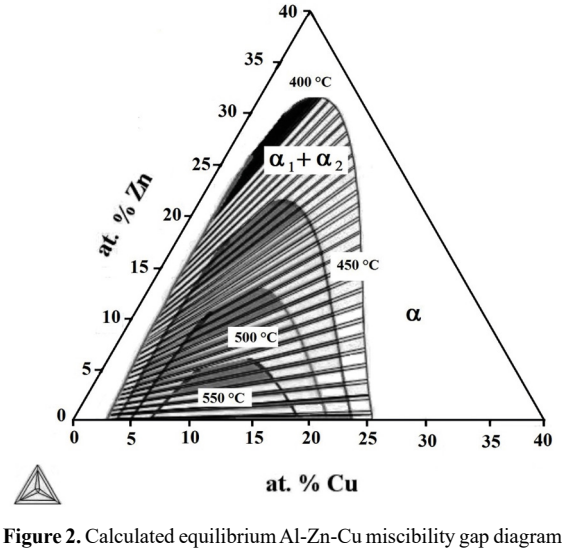

Figure 2. Calculated equilibrium Al-Zn-Cu miscibility gap diagram at different temperatures.

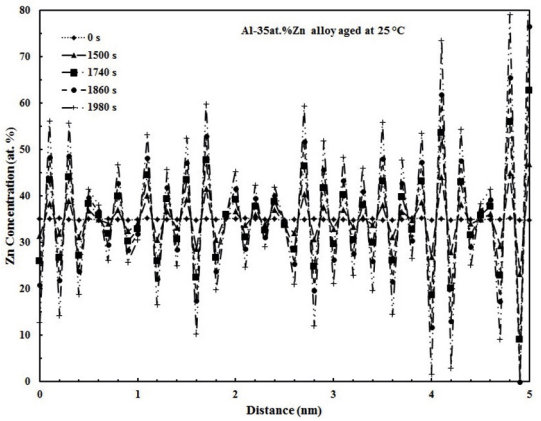

Figure 3. Zn concentration profiles of the Al-35at.%Zn alloy aged at 25 °C for different times.

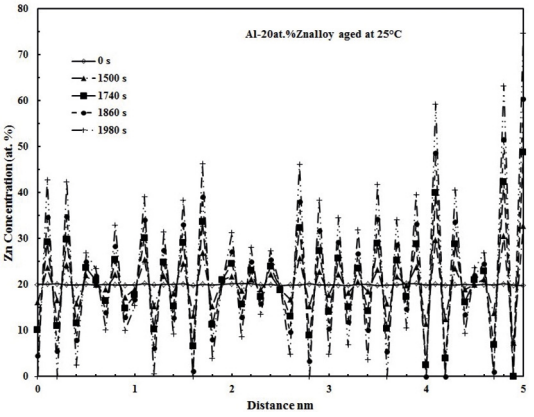

Figure 5. Zn concentration profiles of the Al-20at.%Zn alloy aged at 25 °C for different times.

expected to occur in the spinodal decomposition mechanism. Besides, the initial supersaturated solid solution, curve for 0 s, decomposes into a mixture of Al-rich α_1 and Zn-rich α_2 phases as predicted by the calculated equilibrium diagram of binary system shown in Figure 1. Figure 4 shows the evolution of Zn concentration profiles with aging time for the same composition alloy aged at a higher temperature, 50 °C. The aging time for the start of the spinodal decomposition was considered to be that one corresponding to the initial increase in modulation amplitude, more than ± 2.0 at. %, the initial fluctuation. The start time for this case is much shorter than about 60 s. Furthermore, the aging time was shorter than 10 s in order to cause the spinodal decomposition in the two alloy compositions, Al-20 and 35 at. % Zn alloys aged at temperatures equal to or higher than 100 °C. Hao et al.[17] studied the phase decomposition in an Al-50at.%Zn alloy and they found that the spinodal decomposition proceeded very fast after the solution treatment and quenching, which is in agreement with the present work results.

The evolution of Zn concentration profiles with aging time is shown in Figure 5 for the Al-20at.%Zn alloy aged at 25 °C for different times. The evolution of the modulation amplitude with aging time was higher in the Al-35at.%Zn alloy, Figure 3, than that in the Al-20at.%Zn alloy. This fact can be attributed to the higher driving force of the Al-35at.%Zn alloy which is located almost at the center of the miscibility gap in comparison with the latter alloy composition. This fact suggests a higher value of the amplification factor which promotes a higher evolution of modulation amplitude with time according to the Cahn-Hilliard spinodal decomposition theory[12]. The modulation wavelength remains almost constant with the aging time and it was determined to be between 1.5 and 2.0 nm for example, in the Al-35at.%Zn alloy aged at 25 °C. The modulation wavelength is very short and this can be attributed to the high driving force of the spinodal decomposition in this binary system. This fact, along with the fast atomic diffusion, may be also adopted as the reason for the absence of diffuse zones in the concentration profiles. This characteristic of spinodal decomposition has been widely reported[8-10] to take place during the early stages of aging in different spinodally decomposed alloys. The modulation wavelength values were reported to be about 8-9 nm in the literature[17,18] for the aged Al-Zn alloys by XRD measurements. However, it is difficult to measure it since the spinodal decomposition, sidebands, was already detected in the as-quenched specimens. Muller et al.[19] reported values of about 1 nm for their Monte-Carlo simulation in Al-rich Al-Zn alloys aged at 27 °C for short times, up to 120 s, which shows good agreement with this work result.

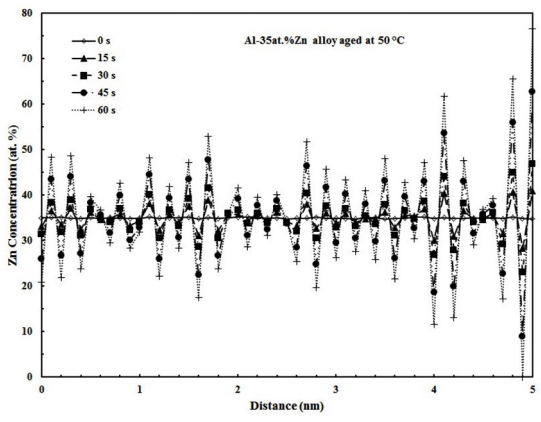

Figure 4. Zn concentration profiles of the Al-35at.%Zn alloy aged at 50 °C for different times.

The morphology of the phase decomposition, determined from the calculated Zn concentration profiles in two dimensions, is shown as an example in Figure 6 for the Al-35at.%Zn alloy aged at 25 °C for 1500 s. The composition scale, 0-50 and 50-100, was selected to show more clearly the Al-rich and Zn-rich phases. The total analyzed area was 20 nm x 20 nm, but this figure only shows a region of 10 nm x 20 nm. This image shows the presence of two phases, Zn-rich (colored in red) and Al-rich (colored in blue), with irregular

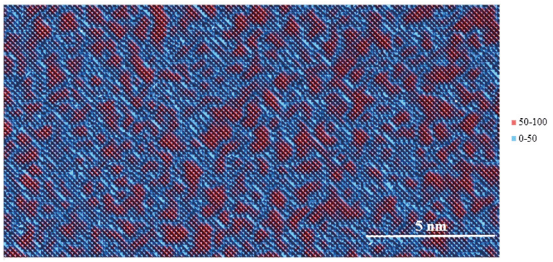

Figure 6. Calculated micrograph of Al-35at.%Zn alloy aged at 25 °C for 1500 s.

and interconnected morphology, which has been reported[7] to occur in spinodally alloys with a low coherency strain-energy and thus no preferential alignment of the decomposed phase can be observed in these alloys. Zn-rich precipitates with an irregular shape were also detected in the Monte-Carlo simulation of aging at 27 °C for up to 120 s in Al-rich Al-Zn alloys[19], which is in agreement with the present work.

As stated before the evidence experimental of phase decomposition is difficult in Al-Zn alloys because of the fast kinetics. Nevertheless, there is a TEM micrograph of the Al-21.2at.%Zn alloy aged at 100 °C for 200 s in the literature[20]. This micrograph shows that the morphology of the decomposed phases is similar to that shown in Figure 6.

3.3 Spinodal decomposition process in Al-Zn-Cu alloys

Figure 7 shows the evolution of Al and Cu concentration profiles with aging time for the Al-20at.%Zn-10at.%Cu alloy aged at 450 °C for different times. The modulation amplitude also increases with aging time which confirms the presence of spinodal decomposition mechanism. Additionally, this figure indicates that the supersaturated solid solution decomposes into a mixture of the Cu-poor Al-Zn α_1 and Cu rich Al-Zn α_2 phases in agreement with the calculated miscibility gaps shown in Figure 2. Furthermore, Thermo-Calc calculation for this alloy composition at 450 °C indicates that the equilibrium composition of the Al-Zn rich α_1 phase is about 90.70 at. % Al, 7.04 at. % Zn and 2.26 at. % Cu, while it is 65.87 at. % Al, 19.63 at. % Zn and 14.5 at. % Cu for the Al-Cu rich α_2 phase, see Figure 2. These values suggest that the Al-Zn rich α_1 phase is Cu-poor, while the Al-Cu rich α_2 phase is Cu-rich. This fact shows a good agreement with the Al and Cu concentration profiles shown in Figure7. This figure also shows that the change in the modulation amplitude with aging time is much slower than that observed in the aged binary alloys, Figures. 3-5, in spite of the higher aging temperature for this ternary alloy. This fact confirms that the copper addition to the Al-Zn alloys delays the spinodal decomposition process. According to the Cahn-Hilliard theory of spinodal decomposition[12], the modulation amplitude is a function of the amplification factor which has to be

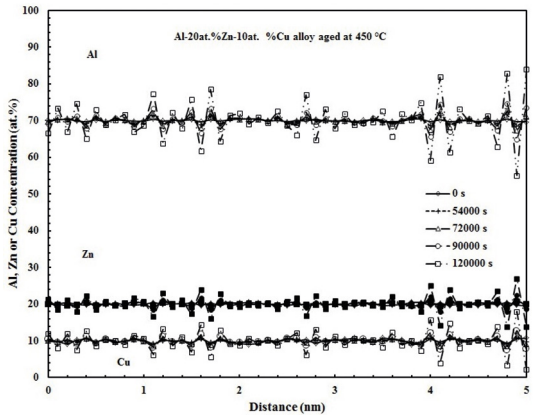

Figure 7. Al, Cu and Zn concentration profiles of the Al-20at.%Zn-10at.%Cu aged at 450 °C for different times.

positive for the spinodal decomposition to take place. The amplification factor is also a function of the atomic mobility. That is, the higher the atomic mobility, the higher value of amplification factor and thus the change in modulation amplitude is faster. This behavior suggests that the copper addition retards the spinodal decomposition process since the atomic mobility or diffusion process is also expected to decrease. Table 2 shows that the activation energy for diffusion of copper in aluminum is higher, 130kJ/mol, than that of zinc in aluminum, 113 kJ/mol,[11] which may confirm the above explained behavior. Experimental results of the 2 at. % Cu addition to an Al-50at.%Zn alloy[17] indicated that the time for the spinodal decomposition increases 20 and 30 times for aging at 300 °C and room temperature, respectively. This retarding behavior is similar to that found in the present work. It is important to point out that the spinodal decomposition may not last as long as predicted in this simulation since several equilibrium phases, not shown in Figure 2, may be formed during the actual aging of Al-Zn-Cu alloys.

The Al, Cu and Zn concentration profiles are shown in Figure 8 for the same composition alloy aged at 425 °C for different times. The modulation amplitude also increases with aging time. The evolution of the spinodal decomposition takes place more slowly than that of the same alloy aged at 450 °C. This is related to the slower diffusive process at 425 °C. Nevertheless, the process evolution is still slower than that observed in the binary aged alloys.

In contrast to the previous results, the evolution of Al concentration profiles for the Al-20at.%Zn-5at.%Cu alloy aged at 450 °C indicates that the spinodal decomposition process is slower than the other alloy aged at the same temperature since the modulation amplitude is lower, as shown in Figure 9. This behavior can be accredited to the lower driving force since this composition is closer to the miscibility gap at this temperature than the other one. The modulation wavelength for the spinodal decomposition in the ternary alloys is slightly shorter, 1.0-1.25 nm, than that

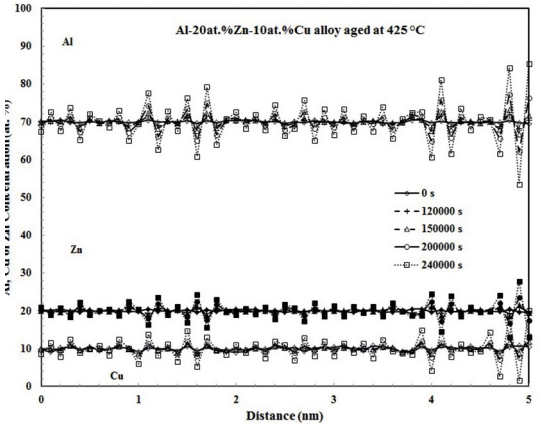

Figure 8. Al, Cu and Znn concentration profiles of the Al-20at.%Zn-10at.%Cu aged at 425 °C for different times.

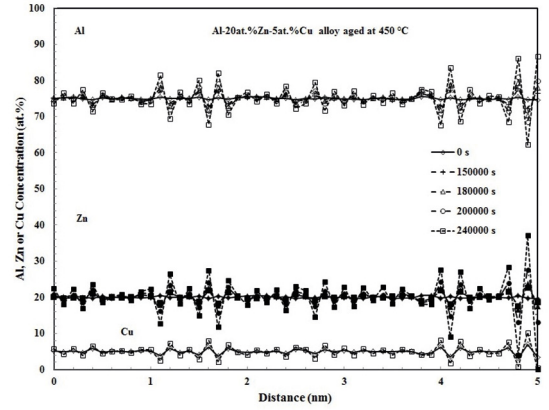

Figure 9. Al, Cu and Zn concentration profiles of the Al-20at.%Zn-5at.%Cu aged at 450 °C for different times.

observed in the binary alloys. Hao et al.[17] also reported similar values for the modulation wavelength in the binary and ternary alloys.

The micrograph of phase decomposition, formed by Zn concentration in two dimensions, is shown in Figure 10 for the Al-20at.%Zn-10at.%Cu aged at 450 °C for 120000 s. Two phases are observed, Al-Zn rich α_1 (green color) and Al-Cu rich α_2 (red color), presenting an irregular and interconnected shape, similar to that observed in the binary alloy. No experimental evidence at high magnifications was found in the literature for the microstructure of the spinodally-decomposed phases during the early stages of aging in the ternary alloys.

4. Conclusions

The copper addition to the Al-Zn alloy system caused the extension of the metastable miscibility gap up to a temperature of about 597 °C for the ternary alloy system. The aging process promoted the spinodal decomposition of the

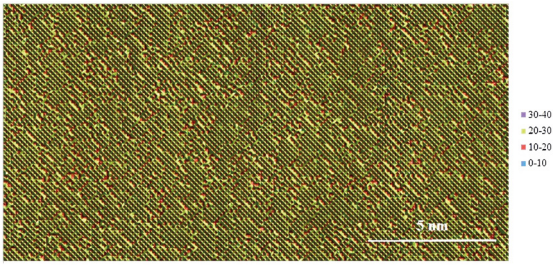

Figure 10. Calculated micrograph of the Al-20at.%Zn-10at.%Cu aged at 450 °C for 120000 s.

supersaturated solid solution in both the binary and ternary alloys. The kinetics of phase decomposition was much faster in the binary alloys than that observed in the ternary in spite of the higher aging temperatures for the latter case. The main characteristics of the spinodal decomposition mechanism were observed to take place in both the aged binary and ternary alloys. The decomposed phases presented an irregular and interconnected shape and they corresponded to the Al-rich α_1 and Zn-rich α_2 phases, and Cu-poor Al-Zn rich α_1 and Cu-rich Al-Zn α_2 phases for the binary and ternary alloys, respectively, as predicted by the corresponding miscibility gaps. Alloy compositions close to the center of miscibility gap exhibited a faster kinetics of phase decomposition.

5. Acknowledgements

The authors wish to acknowledge the financial support from SIP-IPN-CONACYT 220929.

6. References

1. Zhu YH. General Rule of Phase Decomposition in Zn-Al Based Alloys (II) --On Effects of External Stresses on Phase Transformation--. *Materials Transactions*. 2004;45(11):3083-3097.

2. Ren YP, Qin GW, Pei WL, Hao SM. The (α1 + α2) miscibility gap of the Al–Zn–Cu system at 360 °C. *Scripta Materialia*. 2009;61(1):36-39.

3. Dai LL, Li HX, Ren YP. Thermodynamic calculation on the miscibility gap of fcc-Al based solid solution in the Al–Zn–Cu system. *Journal of Alloys and Compounds*. 2009;478(1-2):144-146.

4. Pal HM, Pradhan SK, De M. Microstructure and Mechanical Property of α-Al-Zn-Cu Alloys Aged at Room Temperature. *Materials Transactions, JIM*. 1995;36(4):490-495.

5. Savaşkan T, Pürçek G, Hekimoğlu AP. Effect of Copper Content on the Mechanical and Tribological Properties of ZnAl27-Based Alloys. *Tribology Letters*. 2003;15(3):257-263.

6. Savaşkan T, Alemdağ Y. Effect of nickel additions on the mechanical and sliding wear properties of Al–40Zn–3Cu alloy. *Wear*. 2010;268(3-4):565-570.

7. Miyazaki T. The Forty-Seventh Honda Memorial Lecture - Recent Developments and the Future of Computational Science on Microstructure Formation. *Materials Transactions*. 2002;43(6):1266-1272.

8. Honjo M, Saito Y. Numerical Simulation of Phase Separation in Fe–Cr Binary and Fe–Cr–Mo Ternary Alloys with Use of the Cahn–Hilliard Equation. *ISIJ International*. 2000;40(9):914-919.

9. Soriano-Vargas O, Avila-Davila EO, Lopez-Hirata VM, Dorantes-Rosales HJ, Gonzalez-Velazquez JL. Spinodal Decomposition in an Fe-32 at%Cr Alloy during Isothermal Aging. *Materials Transactions, JIM*. 2009;50(7):1753-1757.

10. Avila-Davila EO, Lopez-Hirata V, Saucedo-Muñoz ML, Gonzalez-Velazquez JL. Microstructural simulation of phase decomposition in Cu–Ni alloys. *Journal of Alloys and Compounds*. 2008;460(1-2):206-212.

11. Mehner H, ed. *Diffusion in Solid Metals and Alloys*. 1st ed. Berlin: Springer-Verlag; 1990. p. 290-291.

12. Hilliard JE. Spinodal Decomposition. In: Aaronson HI, ed. *Phase Transformations*. 1st ed. Metals Park: ASM; 1970. p. 497-560.

13. Pearson WB. *A Handbook of Lattice Spacings and Structures of Metals and Alloys*. 1st ed. New York: Pergamon Press; 1958.

14. www.Thermo-Calc.com, Thermo-Cal software /pbin and ssol5 data bases.

15. Popović S, Gržeta B. Precipitation and Dissolution Phenomena in Al-Zn Alloys. *Croatica Chemica Acta*. 1999;72(2-3):621-643.

16. Ren YP, Chen H, Wang K, Hao SM, Dong DJ. Effect of Cu addition on the α1+α2 miscibility gap of the Al–Zn system. *Scripta Materialia*. 2004;51(3):267-270.

17. S. Hao, Y. Ren, H. Li, D. Wang and G. Zhao, J. Mater. Sci. Technol. 21, 836(2005). Doi: http://www.jmst.org/EN/Y2005/V21/I06/836

18. Douglass DL. Spinodal decomposition in Al/Zn alloys. *Journal of Materials Science*. 1969;4(2):130-137.

19. Müller S, Wang LW, Zunger A. First-principles kinetic theory of precipitate evolution in Al-Zn alloys. *Modelling and Simulation in Materials Science and Engineering*. 2002;10(2):131-146.

20. Miyazaki T, Koyama T, Kozakai T. Computer simulations of the phase transformation in real alloy systems based on the phase field method. *Materials Science and Engineering: A*. 2001;312(1-2):38-49.